

Steady Flow and Dynamic Viscoelastic Behavior of Nylon 1313 Using Parallel-Plate Rheometer and Capillary Rheometer

Yudong Wang,¹ Qingxiang Zhao,¹ Minying Liu,¹ Zhimin Wang,¹ Yukun Liu,¹ Shaokui Cao,¹ Tianzeng Zhao²

¹College of Materials Science and Engineering, Zhengzhou University, Daxue Road, Zhengzhou 450052, People's Republic of China

²Henan Institute of Chemistry, Hongzhuan Road, Zhengzhou 450002, People's Republic of China

Received 3 April 2003; accepted 8 March 2005

DOI 10.1002/app.22261

Published online in Wiley InterScience (www.interscience.wiley.com).

ABSTRACT: In this study, a novel nylon with long alkane segments (also called nylon 1313), which was synthesized using 1,13-tridecanedioic acid in our laboratory, has been characterized. Different rheological behaviors of nylon 1313 have been presented using steady shear, creep recovery, and dynamic tests. The time-temperature effects have also been

investigated. © 2005 Wiley Periodicals, Inc. *J Appl Polym Sci* 98: 1643–1651, 2005

Key words: creep test; nylon 1313; recovery test; rheological properties

INTRODUCTION

Nylon 1313 has 11 methylene units per amide repeat. The advantages of nylons with long alkane segments, such as nylon 11, nylon 12, nylon 1212, nylon 1313, and so forth, include a lower melting point, a slightly lower density, superb toughness, high tensile strength, abrasion resistance, dimensional stability, excellent wet strength retention, and low tissue reaction, plus the lowest dielectric constant and water affinity.^{1–3} The low water absorption of these nylons makes them suitable for uses requiring retention of strength, toughness, abrasion resistance, and electrical properties under varying conditions of humidity.^{4,5} Unfortunately, as far as we are aware, studies of synthesis and characterization of nylon 1313 are rather sparse, and nylon 1313 cannot be mass produced.

Publications on the properties of nylon 1313 are quite limited. The first paper on the synthesis of nylon 1313 based on erucic acid obtained from crambe and rapeseed oil was published in 1967.⁶ In the following year, nylon 1313 made from brassylic acid was reported.^{5,7,8} Wang and coworkers⁹ have characterized nylon 1313 using different instruments and techniques. The crystal of nylon 1313 was found to have a monoclinic form with $a = 4.9\text{\AA}$, $b = 9.22\text{\AA}$, $c = 34.40\text{\AA}$, and $\beta = 121.08^\circ$. The glass transition

temperature is 56°C . The melting temperature measured by DSC at the heating rate of $10\text{K}/\text{min}$ is 174°C . Heat of fusion and amorphous density were estimated to be 230Jg^{-1} and 1.01gcm^{-3} , respectively. Prieto and colleagues¹⁰ have studied the nylon 1313 structure by means of X-rays and electron microscopy. Both X-ray and electron diffraction data, obtained from oriented films as well as from lamellar crystals prepared in solution, evidenced that nylon 1313 adopts a γ structure in a monoclinic lattice of parameters $a^0 = 0.473\text{nm}$, $b^0 = 0.473\text{nm}$, $c^0 = 3.40\text{nm}$, $\alpha = \beta = 90^\circ$, $\gamma = 121^\circ$. Johnson and colleagues¹¹ have investigated treatment-dependent crystal forms of nylon 1313 by x-ray and solid state NMR. They found that two different crystal forms of this polymer could be generated using different methods: a type A form was obtained by extended annealing just below the melting temperature and by film casting from 1,1,1,3,3,3-hexafluoroisopropanol, while a type B form developed on precipitating from *m*-cresol into methanol or film casting from *m*-cresol. Wang and coworkers¹² have studied the morphology and properties of thin films of nylon 1313 casted on water. Film morphology and properties have been characterized by transmission electronic microscopy (TEM), x-ray photoelectron spectroscopy, wide-angle X-ray scattering, differential scanning calorimetry, and contact angle measurements. Using the recently developed technique in our laboratory, a large enough amount of nylon 1313 can be produced for rheological characterization.

Rheological characteristics of polymer melts and polymer solutions are important for both processing and final product quality. There have been no publi-

Correspondence to: Q. Zhao (wyd@zzu.edu.cn).

cations on the rheological properties of nylon 1313 so far. However, the rheological properties of other nylon polymers have been extensively investigated by many authors. Bankar and colleagues¹³ studied rheological properties of nylon 6 at different temperatures. Utracki and coworkers¹⁴ investigated the melt rheology of high density polyethylene polyamide 6 blends. They indicated that a temperature dependent movement of polyamide in the capillary during the extrusion and fibrillation of the polyamide phase in the extensional field occurred at all temperatures. Zhuang and colleagues¹⁵ studied the rheological properties of reinforced nylon 66 composites. Gao and coworkers¹⁶ studied rheological properties of ABS-PA 1010 blends. They reported the compatible ABS-PA 1010 blend has higher viscosity and lower crystallinity compared to the corresponding noncompatible blend.

The rheological properties of nylons with long alkane segments in the molten state have received little study. Information of the rheological properties of the polymer melt is important for design, selection, and operation, involving handling, mixing, storage, and transportation processes. In this article, the rheological measurements in terms of steady shear flow, creep and recovery, and oscillatory stresses are reported for nylon 1313 using both parallel plate rotational and capillary rheometers to obtain information on normal and oscillating stresses. Also, the temperature effect on the behavior of nylon 1313 is discussed over the range of 180–220°C.

EXPERIMENTAL

The rheological experiments were carried out using a Haake RS-150 parallel-plate rheometer and a Haake-II capillary rheometer. The RS-150 has several operating test modes, which are controlled rate (CR) mode, controlled stress (CS) mode, and oscillation (OSC) mode. The RS-150 in the CS mode applies shear stresses to a test sample by means of extremely low inertia. The drive shaft is centered by air bearing to deliver an almost frictionless transmission of the applied stress to the test fluid. The resulting deformation of the tested material is analyzed with a digital encoder that processes 106 impulses per revolution. This resolution makes it possible to measure small shear rates, strains, or yield stress values. The RS-150 can be easily switched between both the CS and CR modes, and it can apply oscillating stress and frequency sweep. A controlled variable lift speed is used to position the upper plate. The plate diameter is 20mm and the gap used is 1mm. Steady shear flow measurements were performed on a capillary rheometer (Haake-II). A capillary with 1mm in diameter and the 40 for length/diameter (L/D) ratio was used. The die was made of tungsten-carbide steel.

The samples of nylon 1313 were prepared by Zhengzhou University with a melting point of 174°C (measured by DSC at a heating rate of 10k/min). The relative viscosity of nylon 1313 measured by dissolving nylon 1313 in 98% vitriol solution at 25°C is 1.91. For proper testing, disk-like specimens were prepared by melting nylon 1313 at the temperature of 230°C for 5min, then compression molding for 10min, to give a 1.5-mm-thick sheet. Prior to testing, the samples were dried under vacuum for 24 h at 85°C to avoid the plasticizing and hydrolyzing effects of humidity on nylon 1313. To prevent degradation of the nylon 1313, the measurements were carried out under a nitrogen atmosphere.

To study the many possible phenomena that could be observed in processes involving the use of nylon 1313 sheets, a wide range of tests was carried out. The tests conducted were steady shear flow, creep recovery, and dynamic behavior. The effects of temperature were studied in the range of 180–220°C. The steady flow behavior tests of nylon 1313 were performed with both the parallel-plate rheometer at lower shear rate ($0.01\text{--}10\text{s}^{-1}$) and the capillary rheometer at higher shear rate ($10\text{--}3000\text{s}^{-1}$) over the range of 180–220°C. The creep-recovery experiments were conducted by applying a constant known value of shear stress to the sample using parallel-plate geometry. The resulting compliance was monitored as a function of time. In the dynamic test, the effect of oscillating stresses or strains on the behavior of the sample was studied.

RESULTS AND DISCUSSION

Steady shear flow

The flow behaviors of nylon 1313 obtained using both the parallel-plate and capillary rheometers are presented in Figures 1 and 2, respectively. The flow curves displayed the relationship between the shear stress (τ) and the shear rate ($\dot{\gamma}$) (Fig. 1). The viscosity curves (Fig. 2) correlated changes in viscosity (η) with the shear rate at three selected temperatures.

Because the lines of shear stress (τ) versus shear rate ($\dot{\gamma}$) at lower shear rate range (a) overlapped each other, the Waterfall Graph (in Microcal Origin version 7.0 pro, Microcal Software, Inc., Northampton, MA) was used to obtain a distinct view. Each dataset was displayed as a line data plot, which was offset by a specified amount in both the X and Y direction. The offset X- and Y-axes are omitted here. From Figure 1, we may see that the stress increases linearly as a function of shear rates. In addition, at lower shear rates [Fig. 1(a)], the viscosity increases almost linearly with the increase of shear rates. This is very similar to many other nylons.^{17–18} From Figure 2(a), we may see that nylon 1313 exhibits pseudoplastic behavior. From

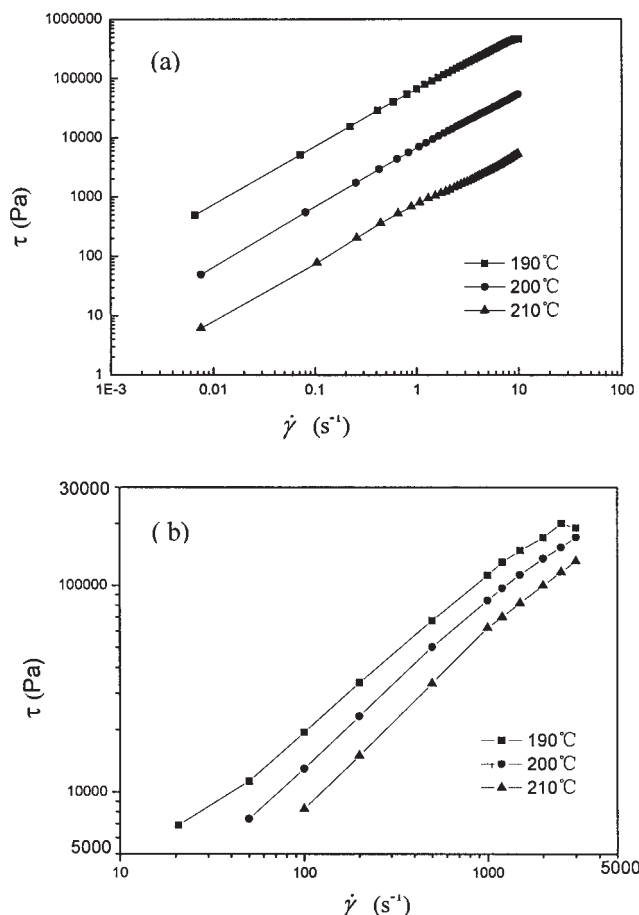


Figure 1 Flow behavior curve of nylon 1313: (a) measured by parallel-plate rheometer (total X offset is 0; total Y offset is 30%); (b) measured by capillary rheometer.

Figure 2(a), we may see that the complex viscosity shows different behaviors under different temperatures. First of all, at lower shear rate range ($\leq 2\text{ s}^{-1}$), the apparent viscosity of nylon 1313 decreased dramatically; however, at higher shear rate range ($> 2\text{ s}^{-1}$), the degree of decrease became slight. These results revealed that the effect of shear rate on the flow behavior of nylon 1313 was more pronounced at lower shear rate compared with its effect at higher shear rate.

The flow behavior of nylon 1313 can be described by the flow curve that, based on a measurement $\tau = f(\dot{\gamma})$, is usually presented in the derived function $\eta = f(\dot{\gamma})$. The experimental measurements of the steady shear flow test were fitted by a nonlinear regression to a Carreau and a power-law model equation:

$$(\eta - \eta_{\infty}) / (\eta_0 - \eta_{\infty}) = [1 + (\lambda \dot{\gamma})^2]^{(n-1)/2} \quad (1)$$

$$\eta = k \dot{\gamma}^{n-1} \quad (2)$$

where η_0 is the zero shear rate viscosity (PaS); η_{∞} the infinite shear rate viscosity (PaS); λ , a time constant (s);

κ , the power-law index (PaS^n); and n , the flow behavior index. The flow curve of nylon 1313 generally is defined by two regions of limited viscosities, η_0 and η_{∞} . At low shear rate, the viscosity approached a constant value of η_0 . As the shear rate enhanced beyond a certain value, viscosity departed from η_0 and became a decreasing function of $\dot{\gamma}$. At a very high shear rate, the molecules of the samples were extended to a maximum limit, and an upper limit viscosity value (η_{∞}) should be reached. Figure 3 displays the relationship between η and $\dot{\gamma}$ based on eqs. (1) and (2). A pretty good linear relation appeared in Figure 3. The regression parameters of eqs. (1) and (2) are listed in Table I. Using the Carreau model, the limiting values of the zero shear viscosity for this study are also reported in Table I; on the other side, the infinite shear rate viscosity of η_{∞} was also obtained at higher shear rate in spite of the shear heating and chain scission that might occur at a very high shear rate.

Table I shows that the nylon 1313 melt experienced strong shear thinning with the increase of shear rates for all temperatures. The effect of temperature on the

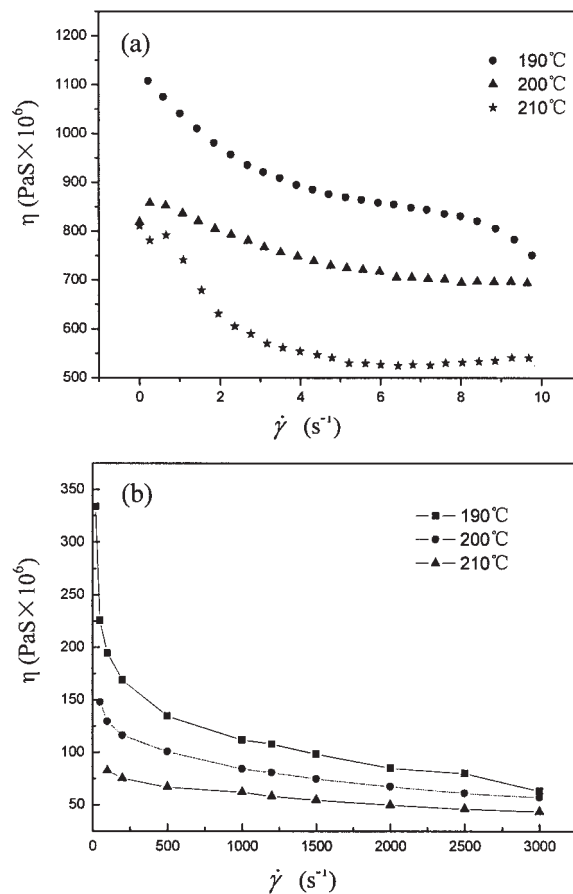


Figure 2 Viscosity curves of nylon 1313: (a) measured with a parallel-plate rheometer; (b) measured with a capillary rheometer.

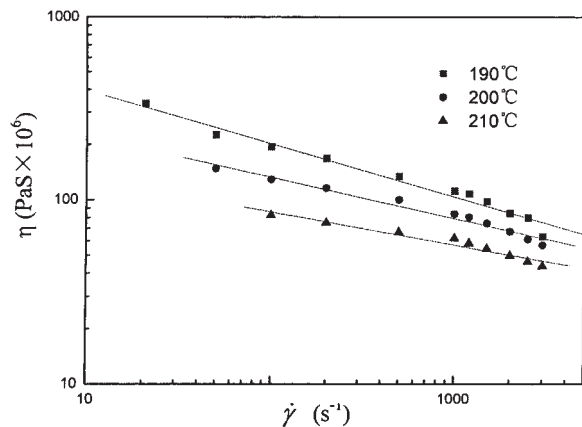


Figure 3 Logarithm viscosity curves of nylon 1313 by means of a capillary rheometer.

viscosity becomes weak with the increase of shear rate. The flow behavior index indicated that the nylon 1313 melt was closer to Newtonian fluid at higher temperatures. In addition, the power-law index of k decreases significantly with the increase of temperature.

Temperature effect

Temperature has a significant influence on viscosity and viscous behavior. It is important to study the flow behavior of nylon 1313 over a wide range of shear rate and temperature. To indicate the sensitivity of the melt viscosity of nylon 1313 to the temperature, the melt viscosity of the sample was measured in the range of temperature of 180–220°C.

Figure 4 shows the relationship between the shear viscosity of nylon 1313 and temperature in the range 180–220°C at different shear rates. There was a significant decrease in the apparent viscosity of nylon 1313 with temperature. The effect of temperature was more pronounced at lower temperature compared with its effect at higher temperature. On the other hand, the viscosity of nylon 1313 showed a dramatic decrease with the increase of shear rate. This could be due to the shear-thinning behavior of nylon 1313 with the

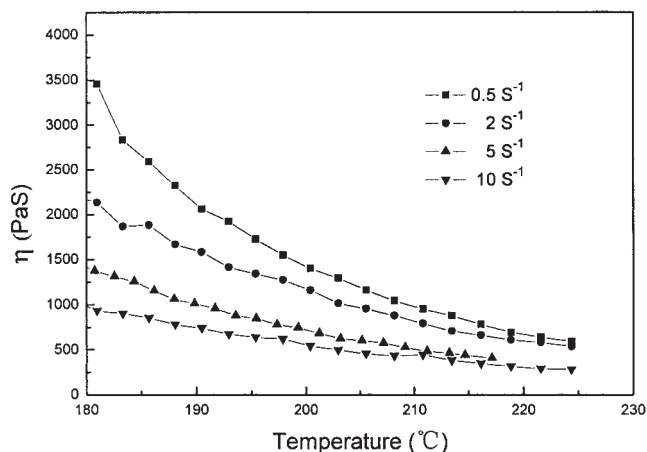


Figure 4 Effects of temperature on the viscosity of the nylon 1313 melt at different shear rates.

increasing of shear rate. According to the Arrhenius equation:

$$\eta = A \exp(-E_a/RT) \quad (3)$$

$$\ln \eta = \ln A - E_a/RT \quad (4)$$

where η is the melt viscosity and E_a is the activation energy for the melt flow.

We made a plot of $\ln \eta$ versus $1/T$ based on eq. (4) (Fig. 5) and calculated the activation energy (E_a) for the melt flow according to the slope of the straight line. The results are shown in Table II.

From Table II, we could see that the viscous flow activation energy was higher at lower shear rate; however, the viscous flow activation energy was much lower at higher shear rate. So, we can understand that the apparent viscosity was sensitive to temperature at lower shear stress because of higher activation energy (E_a), and the temperature effect on the apparent vis-

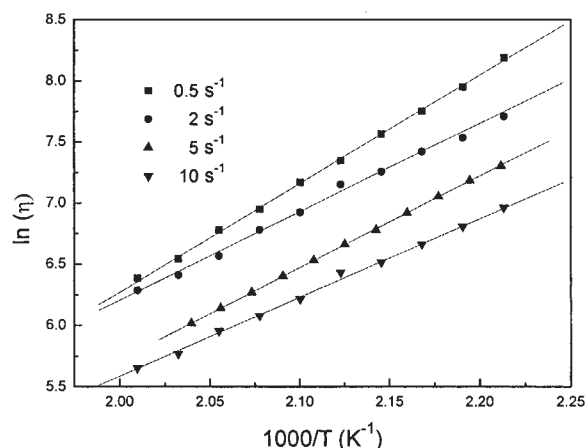


Figure 5 Apparent activation energy for the melt flow of nylon 1313 at different shear rates.

TABLE I
Zero Shear Viscosity (η_0), Flow Behavior Index (n), Infinite Shear Rate Viscosity (η_∞), and Power-law Index (k) for Nylon 1313

Temperature (°C)	η_0	n	η_∞	k
190	1181	0.71	63.4	17.92
200	862.5	0.78	57.1	13.10
210	810	0.82	43.7	9.94

TABLE II
Results of Apparent Activation Energies for Different Shear Rates

Shear rate (s^{-1})	Activation energy (E_a)	R
0.5	73.87	0.999
2	60.20	0.998
5	62.41	0.999
10	53.39	0.997

cosity became weaker at higher shear stress because of lower activation energy (E_a). This phenomenon could also be observed clearly from Figure 4.

Creep-Recovery test

To reveal the viscoelastic characteristics of a polymer melt, a sample should be tested for its response to a constant stress over time. Polymer melts that exhibit viscoelastic behavior have long chain molecules, which at rest loop and entangle with each other at a minimum-energy state. Under deformation, these molecules stretch, increasing the bond vector angles and raising their energy state. If the cause of deformation is removed, the molecules try to return to their original energy state. In pure elastic behavior, the deformation response to a constant shear stress τ is linearly linked to its value and is maintained as long as the stress is applied. The deformation will disappear completely and simultaneously when the stress is removed. A viscoelastic response to an applied constant stress varies with the time of application. Initially, the network of molecules undergoes deformation within the mechanical limits of the network. Continuous deformations lead to dismantling of the network, and the polymer melt starts to flow. When the applied stress is removed, the total strain separates into a permanently maintained viscous part and a recovery elastic part. Viscoelastic behavior under lower values of stress usually has a linear response. In the range of nonlinear responses, at higher stress values, elasticity and viscosity data are usually dependent on the test conditions and the sensor system parameters.

Rheological systems that exhibit creep show a time-dependent strain $\gamma(t)$ under a constant stress τ , where:¹⁹

$$\gamma(t) = J(t) \times \tau \quad (5)$$

The compliance, $J(t)$ (Pa^{-1}), of a sample is a material constant. The higher the compliance, the easier the sample can be deformed by a given stress. In the linear viscoelastic range, the compliance is independent of the applied stress. Consequently, the proper creep and

recovery test conditions within the limit of linear viscoelasticity can be defined. In addition, linear viscoelasticity is a nondestructive test of measuring the rheological behavior of a sample. The deforming energy is recovered when the applied stress is released. This indicates the network ability to elastically deform while keeping the network intact.

In the creep-recovery test, it was important to initially define the linear viscoelastic range by applying different values of constant shear stress for 120 s. The strain data $\gamma(t)$ at different values of applied shear stress should coincide within the linear viscoelastic range. However, in the nonlinear viscoelastic range, the strain data curve separated significantly from the linear viscoelastic data. So, a creep test carried out to define the linear viscoelastic range for the nylon 1313 melt was very important. It was determined that the linear viscoelastic ranges for nylon 1313 at the range of temperature 180–220°C was in the neighborhood of 15 Pa.

The creep-recover experiments were conducted by applying a constant known value of shear stress (within the linear range) to the sample using the parallel-plate rheometer. The resulting compliance and strain were monitored as a function of time. The imposed stress was suddenly removed after 120s, and recovery was monitored for 200s. Figure 6 shows the strain data $\gamma(t)$ for nylon 1313 at different temperatures for a given stress. Figure 7 shows the strain data $\gamma(t)$ for nylon 1313 at different shear stresses for a fixed temperature. For nylon 1313, a noticeable time-dependent response was evident in the creep and recovery phases at lower applied shear stress. Therefore, nylon 1313 showed an elastic recovery in addition to its viscous response at lower applied shear stress. However, at higher applied shear stress, the time dependence in the creep phase was diminished and was significantly reduced in the recovery phase. The re-

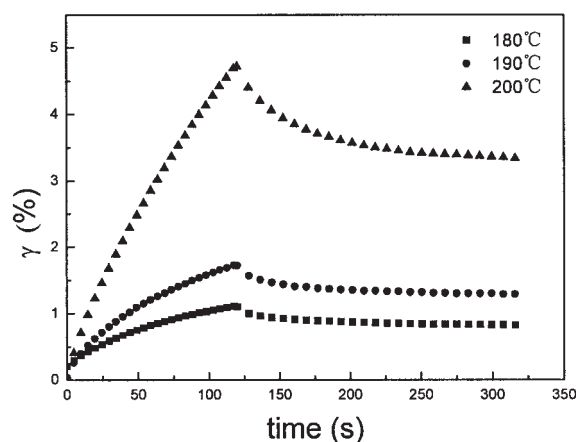


Figure 6 Viscoelastic response of nylon 1313 at a fixed stress of 10 Pa.

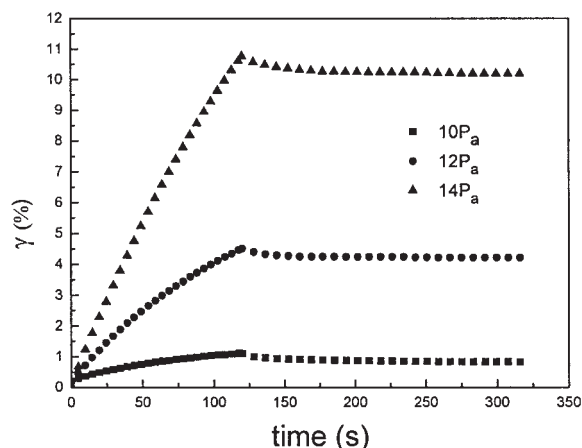


Figure 7 Viscoelastic response of nylon 1313 at a fixed temperature of 180°C.

sponse of the strain $\gamma(t)$ to the instantaneous removal of stress could be summarized into three steps: Initially, a step reduction occurred as a pure elastic response, followed by an exponential decrease related to a viscoelastic response. Finally, the strain values approached a constant limit corresponding to the nonrecovered deformation of the viscous flow. The elastically stored deformation energy will reduce the maximum strain of the first creep phase. The recovery curve of the second phase will drop towards the abscissa and eventually reach a constant strain level. The difference between the strain maximum and this constant recovery strain level was the elastic recovery of the tested material. The difference between that constant recovery strain level and the abscissa described the amount of unrecoverable strain corresponding to viscous flow. Figure 7 indicates that with increasing stress in the first phase, the recovery increased. In addition, the same phenomenon was observed in Figure 6, namely, with enhancing the temperature the recovery increased. This revealed that the effect of stress and temperature on the creep and recovery was consistent over the discussed range of stress and temperature.

For comparison, Figure 8 shows the strain values of nylon 1313 at 200°C for different shear stress values in the nonlinear viscoelastic range. From Figure 8 we can see that nylon 1313 exhibited time-independent behavior in the creep and recovery phases. Also, a pure viscous response of nonrecovered deformation could be seen. This is significantly different from the behavior recovered in the linear viscoelastic range in Figures 6 and 7.

Dynamic test

The dynamic test is another tool of rheological study of viscoelastic behavior. In this test, the effect of oscil-

lating stresses or strains on the behavior of the sample was studied. In the controlled stress mode, the stress may be applied as a sinusoidal time function:

$$\tau = \tau_0 \sin(\omega t) \quad (6)$$

The approach taken in the dynamic test to study the viscoelastic behavior is different from the approach of the creep-recovery test. The two tests complement each other, since some features of viscoelasticity are better described in a creep-recovery test and others in a dynamic test.

The complex modulus $G^*(P_a)$ represents the substance total resistance against the applied strain and can be calculated from

$$G^* = \tau_0 / \gamma_0 \quad (7)$$

where τ_0 and γ_0 are the stress and strain amplitudes, respectively. On the other hand, it can be defined as:

$$G^* = G' + iG'' \quad (8)$$

where G' and G'' are the storage modulus and loss modulus, respectively. Complex viscosity represents the total resistance to a dynamic shear as

$$\eta^* = G^* / \omega \quad (9)$$

where ω is the frequency (rad/s) and η^* is the complex viscosity (mPas). To determine the linear viscoelastic range in a dynamic test, a fixed frequency 1 Hz is used while a stress sweep is performed. The stress is automatically increased to cover a wide range. The linear viscoelastic range is the range where $G^*(P_a)$ is constant with the stress (τ). At higher stress, the sample structure is deformed to the point that the internal temporary bonds are destroyed. Shear thinning will take

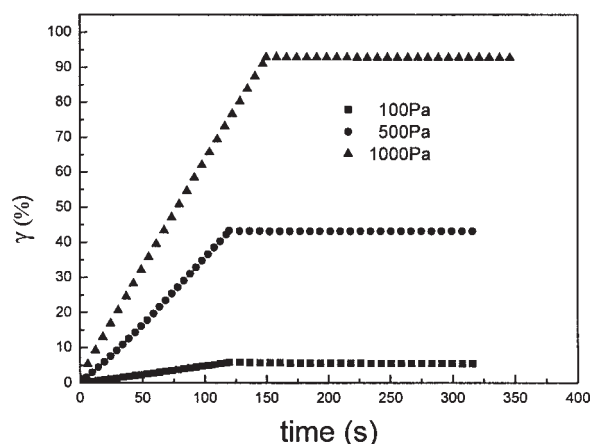


Figure 8 Viscoelastic response of nylon 1313 in a nonlinear viscoelastic range at 200°C.

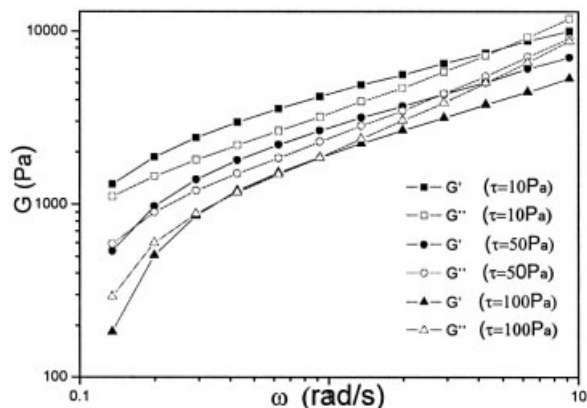


Figure 9 G' and G'' for nylon 1313 at different shear rates for the fixed temperature of 200°C.

place, and a major part of the introduced energy will irreversibly be lost as heat. In the linear range of viscoelasticity, the relevant equations are linear differential equations with constant coefficients. Dynamic tests must start with a stress sweep to determine the linear viscoelastic range. Then, further tests can be performed to determine features of the viscoelastic behavior. The linear viscoelastic range for nylon 1313 at the range of temperature 180–220°C was found to be in the neighborhood of 100 Pa.

The rheological properties of nylon 1313 were measured using an oscillatory shear rheometer with parallel-plate geometry in the frequency range of 0.1–10 rad/s. The storage modulus (G') and the loss modulus (G'') in the linear viscoelastic range at different stresses and different shear temperatures were plotted in Figures 9 and 10, respectively. In Figures 9 and 10, the following tendencies are observed: increasing the stress and temperature moved the crossover point of G' to G'' to lower frequencies; in the meantime, the values of G' and G'' decreased under the discussed

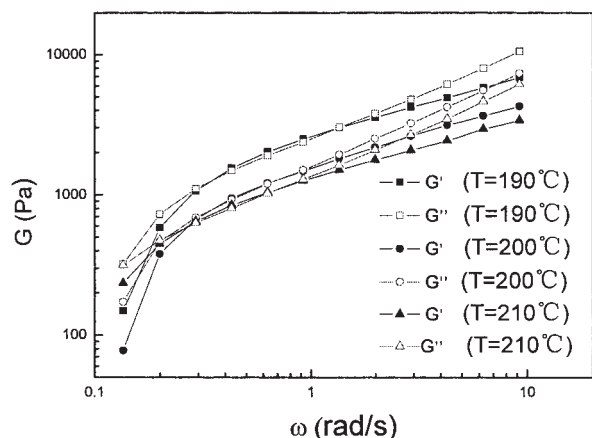


Figure 10 G' and G'' for nylon 1313 at different temperatures for the fixed shear rate of 100 Pa.

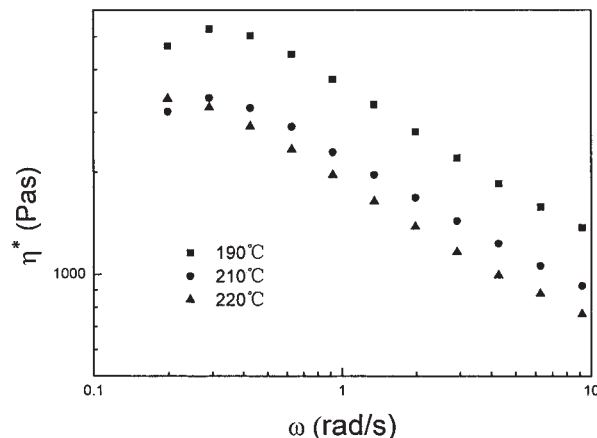


Figure 11 Complex viscosity-frequency of nylon 1313 at different temperatures.

stresses and temperatures. From Figure 9 we can see that with the increasing of stress, the elastic response becomes weaker than the viscous response. When the shear stress increased to 100 Pa, the viscous behavior was more predominant than the elastic behavior. At lower angular velocities, the G' curve was well above the G'' curve in addition to the curve at the stress of 10 Pa, indicating that the viscous behavior was superior to the elastic one at a lower range of frequency. With the increasing of angular velocities, the elastic response indicated by G' exceeded the viscous one of G'' , except the curve at the shear stress of 100 Pa. For even higher angular speeds, the two curves of the moduli crossed over at a particular value of the angular velocity, which was characteristic for the polymer structure. Subsequently, the viscous response exceeded the elastic response, indicating that the viscous behavior was more predominant at a higher range of frequency. The similar phenomenon could be observed in Figure 10. In addition, Figures 9 and 10 indicated that the frequency range responsible for elastic behavior decreases with the increase of temperature and shear stress. This conclusion is in very good agreement with the behavior of the creep-recovery response.

The complex viscosity of nylon 1313 is shown in Figure 11 versus the frequency in the range of 0.1–10 rad/s. Steady shear viscosity or oscillating viscosity can be used for polymer fluids characterization. Similarities between steady shear viscosity and dynamic viscosity exist as reflected by

$$\lim_{\dot{\gamma} \rightarrow 0} \eta(\dot{\gamma}) = \lim_{\omega \rightarrow 0} \eta(\omega) \quad (10)$$

where η is the real component of the dynamic viscosity. This relation was predicted by a molecular study.¹⁷ Many polymer fluids have been found to

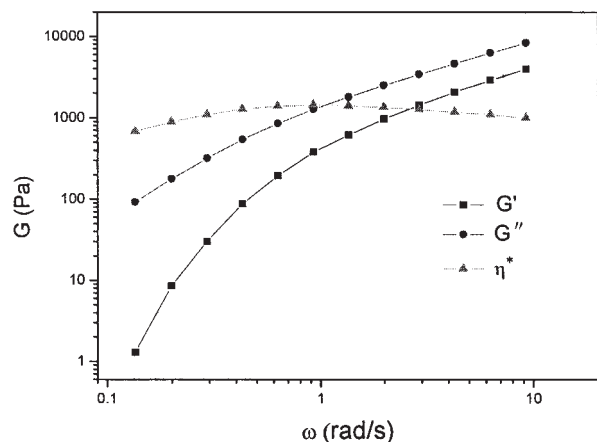


Figure 12 Dynamic viscoelastic behavior of nylon 1313 at the nonlinear viscoelastic range ($\tau = 1000$ Pa, $T = 200^\circ\text{C}$).

follow eq. (10) experimentally. At a higher shear rate, deviations from eq. (10) are usually observed (i.e., η decreases more rapidly with ω than η decreases with $\dot{\gamma}$). Cox and Merz²⁰ found a useful empirical relationship that predicts that the complex dynamic viscosity (η^*) should be identical to the steady shear viscosity at equal values of ω and $\dot{\gamma}$:

$$\eta^*(\omega) = \eta(\dot{\gamma}) \quad (11)$$

Figure 11 denotes that the dynamic viscosity decreased with the frequency for all the selected temperatures displaying a shear-thinning behavior. The viscosity curves showed a Newtonian range at low frequencies and then started to decrease; the complex viscosity exhibited a very similar behavior to the dynamic viscosity of steady-state flow, which also revealed shear-thinning at higher shear rates. On the other hand, the temperature has a significant influence on the dynamic viscosity of the nylon1313 melt. With the increase of temperature, the complex viscosity decreased. In addition, comparing Figures 2 and 11 it could be revealed that the complex dynamic viscosity was higher than the shear viscosity for all the tested temperatures due to the energetic interaction of hydrogen bonds on the internal structure of the nylon 1313 molecules.²¹

For comparison, Figure 12 displays the dynamic viscoelastic behavior of nylon 1313 in the nonlinear viscoelastic range. Figure 12 indicates that the loss modulus was higher than the storage modulus over the whole range of frequency, indicating that viscous behavior was more predominant at the nonlinear viscoelastic range. Also, the complex viscosity almost kept parallel with the abscissa. This is to say that the nylon 1313 melt shows close to Newtonian fluid behavior at the higher applied shear stress range.

CONCLUSIONS

A comprehensive rheological study for nylon 1313 melt was carried out using a parallel-plate rheometer and a capillary rheometer. The nylon 1313 melt showed shear-thinning behavior for all the temperatures. The flow behavior index under different temperatures was obtained. The experimental trial showed that the nylon 1313 melt belongs to pseudo-plastic fluid, with the flow behavior index less than 1. In the low and in the high shear rate ranges, the first and the second Newtonian behaviors were observed—even the viscosity of non-Newtonian fluid is independent of shear rate.

The effect of temperature on the flow behavior was investigated at different shear rates. The activation energy is high at lower shear rates; however, the viscous flow activation energy was much lower at higher shear rates. The temperature effect on the apparent viscosity became weaker at higher shear stress because of lower activation energy (E_a).

A creep-recovery test was carried out to define the linear viscoelastic range as 15 Pa for the temperature range 180–220°C. A time-dependent response was found for the creep and recovery phases at lower constant applied shear stresses. However, at higher shear stresses, the creep and recovery phases were time-independent.

Dynamic tests were carried out to reveal the viscoelastic behavior of the nylon 1313 melt. The linear viscoelastic range for all tested temperatures according to these tests was 100 Pa. The nylon 1313 melt showed viscous behavior at a very low range of frequency except the lower applied stress (lower than 10 Pa). With the increasing of angular velocities, the elastic response indicated by G' exceeded the viscous one of G'' for specific frequency ranges. For even higher angular speeds, the viscous response exceeded the elastic response, indicating that the viscous behavior is more predominant at a higher range of frequency. The viscoelastic behavior of the nylon 1313 melt depends strongly on the temperature and the applied stress over the range 180–220°C. The complex viscosity was measured over 0.1–10 rad/s and showed a shear-thinning behavior with frequency and temperature dependence.

The Scientific Project of Henan Province sponsored this work (0424270081).

References

1. Li, Q. F.; Tian, M.; Kim, D. G.; Wu, D. Z.; Jin, R. G. *J Appl Polym Sci* 2002, 83, 1600.
2. Davis, R. D.; Jarrett, W. L.; Mathias, L. J. *Polymer* 2001, 42, 2621.
3. Jones, N. A.; Atkins, E. D. T.; Hill, M. J.; Cooper, S. J.; Franco, L. *Macromolecules* 1997, 30, 3569.

4. Kohan, K. I. *Nylon Plastics*; Wiley-Interscience: New York, 1973.
5. Perkins, R. B.; Roden III, J. J.; Tanquary, A. C.; Wolff, I. A. *Mod Plastics* 1969, 5, 136.
6. Wolff, I. A. *The Encyclopedia of Basic Materials for Plastics*, Reinhold Publishing Corp.: New York, 1967.
7. Donald, L. V. D.; Melvin G. B. *Biotechnol Prog* 1969, 6, 273.
8. Kestler, J. *Mod Plastic* 1968, 45, 86.
9. Wang, L.-H.; Calleja, F. J. B.; Kanamoto, T.; Porter, R. S. *Polymer* 1993, 34, 4688.
10. Prieto, A.; Iribarren, I.; Munoz-Guerra, S. *J Mater Sci* 1993, 28, 4059.
11. Johnson, C. G.; Mathias, L. J. *Polymer* 1993, 34, 4978.
12. Wang, L. H.; Porter, R. S. *J Polym Sci Part B: Polym Phys* 1995, 33, 785.
13. Bankar, V. G.; Spruiell, J. E.; Wite, J. L. *J Appl Polym Sci* 1977, 21, 2135.
14. Utracki, L. A.; Dumoulin, M. M.; Toma, P. *Polym Eng Sci* 1986, 26, 34.
15. Zhuang, G. Q.; Gui, Y.; Yang, Y. M.; Li, B. Y.; Zhang, J. X. *J Appl Polym Sci* 1998, 69, 589.
16. Gao, G.; Wang, J. Y.; Yin, J. H.; Yu, X. Q. *J Appl Polym Sci* 1999, 72, 683.
17. Carreau, P. J. *Trans Soc Rheol* 1972, 16, 99.
18. Parrini, P.; Romanini, D.; Righi, G. P. *Polymer* 1976, 17, 377.
19. Mohamed, E.; Esmail, N. M.; Vatistas, G. H. *J Appl Polym Sci* 2001, 79, 1787.
20. Cox, W.; Merz, E. *J Polym Sci* 1958, 28, 619.
21. Kulicke, W.; Kniewske, R.; Klein, J. *Prog Polym Sci* 1982, 8, 373.